Neoplasia • Vol. 7, No. 9, September 2005, pp. 824–837 824

www.neoplasia.com

TWIST is Expressed in Human Gliomas and Promotes Invasion[1]

Maria C. Elias[*,2], Kathleen R. Tozer*[*,2], John R. Silber*, Svetlana Mikheeva*, Mei Deng*, Richard S. Morrison*, Thomas C. Manning*, Daniel L. Silbergeld*, Carlotta A. Glackin[†], Thomas A. Reh[‡] and Robert C. Rostomily**

*Department of Neurological Surgery, University of Washington, Seattle, WA 98195, USA; [†]Department of Molecular Medicine, City of Hope Beckman Research Institute, Duarte, CA 91010, USA; [‡]Department of Biological Structure, University of Washington, Seattle, WA 98195, USA

Abstract

***TWIST* is a basic helix–loop–helix (bHLH) transcription factor that regulates mesodermal development, promotes tumor cell metastasis, and, in response to cytotoxic stress, enhances cell survival. Our screen for bHLH gene expression in rat C6 glioma revealed *TWIST*. To delineate a possible oncogenic role for TWIST in the human central nervous system (CNS), we analyzed *TWIST* message and protein expression in gliomas and normal brain. *TWIST* was detected in the large majority of human glioma–derived cell lines and human gliomas examined. Increased *TWIST* mRNA levels were associated with the highest grade gliomas, and increased *TWIST* expression accompanied transition from low grade to high grade *in vivo*, suggesting a role for TWIST in promoting malignant progression. In accord, elevated *TWIST* mRNA abundance preceded the spontaneous malignant transformation of cultured mouse astrocytes hemizygous for p53. Overexpression of TWIST protein in a human glioma cell line significantly enhanced tumor cell invasion, a hallmark of high-grade gliomas. These findings support roles for *TWIST* both in early glial tumorigenesis and subsequent malignant progression. *TWIST* was also expressed in embryonic and fetal human brain, and in neurons, but not glia, of mature brain, indicating that, in gliomas, *TWIST* may promote the functions also critical for CNS development or normal neuronal physiology.**

Neoplasia (2005) **7,** 824–837

Keywords: cancer, brain tumor, neuron, oncogene, invasion.

Introduction

The basic helix–loop–helix (bHLH) family of proteins regulates normal development and differentiation by forming DNA-binding heterodimers composed of tissue-specific (class B) and ubiquitously expressed (class A) proteins that direct cell-specific gene expression [1,2]. The class B bHLH protein, TWIST, plays a central role in determining cell fate in mesoderm, primarily during myogenesis [3–6]. For example, *TWIST* prevents development in normal skeletal muscle by forming inactive heterodimers with other myogenic bHLH proteins (e.g., MyoD and myogenin) that direct the acquisition of a quiescent, differentiated phenotype [7–9]. *TWIST* also inhibits the induction of p53-mediated apoptosis in rodent fibroblasts in response to genotoxins and prolonged serum deprivation [10]. Both functions of *TWIST* are likely essential for normal development as evidenced by death *in utero* at embryonic day 11.5 in *TWIST* null mice accompanied by a high frequency of apoptotic cells [3].

The antiapoptotic function of *TWIST* suggests that it could function as an oncogene [10]. In accord, elevated levels of *TWIST* mRNA have been observed in the mesenchymal tumors, rhabdomyosarcoma and osteosarcoma [10,11]. The recent demonstration of oncogenic cooperation between *TWIST* and N-myc amplification in neuroblastoma [12] and *TWIST* expression in a variety of carcinomas [11,13,14] supports an oncogenic function that is not limited to mesenchymal-derived neoplasms. *TWIST* expression in gastric carcinoma [13] has been associated with the initial phase of the metastatic process whereby tumor cells transition from an epithelial to an invasive mesenchymal phenotype. Indeed, in a mouse breast carcinoma model, *TWIST* is necessary for cells to metastasize by promoting this epithelial mesenchymal transition (EMT) and inducing cell motility [15]. Notably, elevated levels of *TWIST* mRNA correlate with invasive breast cancer phenotype [15]. Thus, *TWIST* promotes increased tumor cell survival and motility—two features characteristic of malignant gliomas. To our knowledge, *TWIST* expression has not been characterized in human primary brain tumors.

Human adult gliomas arise from mature glia and/or glial progenitors in the brain [16]. Classified histologically in order of increasing malignancy from grades II to IV, gliomas can

Abbreviations: bHLH, basic helix–loop–helix; CNS, central nervous system; FBS, fetal bovine serum; GBM, glioblastoma; GS, gliosarcoma; H&E, hematoxylin and eosin; HGF, hepatocyte growth factor; IGF, insulin-like growth factor

Address all correspondence to: Robert C. Rostomily, MD, Department of Neurological Surgery, Box 356470, University of Washington, 1959 NE Pacific Street, Seattle, WA 98195-6470. E-mail: rosto@u.washington.edu

[1]This work was supported by National Institutes of Health grants KO8 NS02217 (R.C.R.), NS42123 (R.S.M.), CA82622 (J.R.S.), NS28308 (T.A.R.), and T32-NS00714424 (UW Department of Neurological Surgery). Additional support was provided by grants from The Seattle Foundation (R.C.R.) and University of Washington HHMI Pilot Study (R.C.R.).

[2]Maria C. Elias and Kathleeen R. Tozer contributed equally to the manuscript.

Received 27 May 2004; Revised 21 April 2005; Accepted 18 May 2005.

DOI 10.1593/neo.04352

develop *de novo* as grade IV neoplasms (glioblastoma multiforme) or can undergo malignant progression from low-grade (grade II) or anaplastic gliomas (grade III) to "secondary" glioblastomas [17,18]. Importantly, as tumors increase in grade, they also demonstrate enhanced cell survival accompanying loss of apoptosis in response to cytotoxic insult, increased tumor cell migration and invasiveness, increased cell proliferation, and induction of tumor angiogenesis [19–21]. As noted above, in other cell types or cancers, the regulation of many hallmark behaviors of gliomas has been attributed to *TWIST*.

Here we examine *TWIST* mRNA and protein expression in human glioma–derived cell lines, glioma tissues, and normal developing and mature brains, and also in an *in vitro* model of glial tumorigenesis using mouse p53-deficient astrocytes [22–24] to further characterize possible associations with gliomagenesis or glial tumor progression. We also examine the contribution of *TWIST* to the phenotype of human glioma cells by analyzing the effect of *TWIST* overexpression on invasion in a glioma cell line. Our data support functions for *TWIST* that contribute to glial tumorigenesis and glioma tumor cell behavior, as well as potential roles in the developing and mature human central nervous system (CNS).

Materials and Methods

Cell Lines and Tissues

Cell lines studied were derived from glioblastoma (C6, SNB19, UW18, UW455, UW456, UW467, U87, U138MG, U373MG, SF763, SF767, A172, and T98G), neuroblastoma (SKNMC and IMR32), medulloblastoma (D283), and colorectal (SW480 and HT29), breast (MDA231 and MDA453), and small cell lung cancer (SCLC; H82 and H209). Lines with the UW designation were established in the authors' laboratories and grown in DMEM/F12 with 10% fetal bovine serum (FBS). The remaining cell lines were either obtained from the Brain Tumor Research Center Tissue Bank (SF767 and SF763; Department of Neurological Surgery, University of California, San Francisco, CA) or purchased from the American Type Culture Collection (ATCC; Manassas, VA), and were cultured as recommended. All human tissues were obtained in accordance with human subjects protocols approved by the University of Washington Institutional Review Board. Tumor and normal brain specimens were obtained with informed consent from adult patients operated for glioma, and epilepsy or benign nonglial tumors, respectively. Clinical and demographic data including pathologic diagnosis and tumor grade (based on clinical neuropathology reports), recurrence status, and prior therapy were noted for each patient. Adult samples were snap-frozen in liquid nitrogen and stored at −80°C. At the time of RNA extraction, a portion of each sample was cut and processed for hematoxylin and eosin (H&E) histology. Fetal tissues, obtained from the University of Washington Birth Defects Research Laboratory, Department of Pediatrics (Seattle, WA), were examined and carefully dissected to include only CNS tissues.

Degenerate Reverse Transcription Polymerase Chain Reaction (RT-PCR) Cloning

Degenerate RT-PCR cloning was utilized to identify novel class B bHLH genes expressed in the rat C6 glioma cell line. The design of the degenerate primers was based on conserved class B–specific sequences within the bHLH region as previously described [25]. PCR products were cloned into pCR2.1-TOPO vector with the TOPO-TA system according to the manufacturer's instructions (Invitrogen, Carlsbad, CA), and individual clones were sequenced to identify bHLH genes. A probe generated from the insert of the *TWIST* clone was used for Northern blot confirmation of *TWIST* expression in the C6 glioma cell line according to methods described below.

Northern Blot Analysis

Twenty microgram of total RNA was analyzed for steady-state levels of *TWIST* mRNA by Northern blot analysis using previously published methods [26]. *TWIST* probe was generated from a cloned 556-bp fragment from the 3′ end of the gene using the Megaprime DNA labeling system (Amersham Pharmacia, Piscataway, NJ) with ^{32}P-labeled dCTP. Images of ethidium-stained 18S and 28S RNA bands were obtained before and after transfer to confirm loading, RNA integrity, and complete transfer.

TWIST *Expression Constructs and Cell Transfection*

The human *TWIST* cDNA clone (GenBank ID BC036704) was purchased from ATCC. Open reading frame (ORF) was amplified with PCR primers: 5′-cgccaccatgatgcaggacgtgtccagctcg-3′ and 5′-actagtgggacgcggacatggaccag-3′. The upstream primer was designed with Kozak sequence [27] for improved protein translation. The resulting PCR product was subcloned into pCR2.1-TOPO vector (Invitrogen) and verified by sequencing. The *Eco*RI fragment was then subcloned into the *Eco*RI site of the pLXSN retroviral vector (BD Biosciences, San Jose, CA). Following sequence verification, the *TWIST* expression construct or empty vector was transfected into packaging Phoenix cells in serum-free DMEM/F12 using Lipofectamine Plus reagent (Invitrogen) according to the manufacturer's recommendations. Twelve hours later, the medium was replaced with medium containing 10% FBS. Following an additional 24 hours of incubation, the medium containing virus was collected, filtered through a PVDF filter, and used for infection of SF767 cells in the presence of 4 μg/ml Polybrene (Sigma, St. Louis, MO). Selection of infected cells was begun after 48 hours by culturing cells in the presence of G418 (Sigma). Pools of G418-resistant SF767 cells were collected and expanded, and endogenous expression of TWIST protein was confirmed by Western blot analyses. Cells overexpressing *TWIST* are designated SF767Tw and empty vector controls SF767 LXSN.

TWIST *Antibody*

Twenty one amino acids (SSGGGSPQSTEELQTQRVMA) specific for TWIST-1 protein near the loop region of the HLH domain were chemically synthesized and conjugated with a carrier, Keyhole limpet hemocyanin. After high-performance

liquid chromatography (HPLC) analysis to determine Keyhole limpet hemocyanin binding efficiency and peptide purification, the protein antigen was injected into three rabbits for immunization. The specificity of the peptide sequence for *TWIST* and the lack of homology to other related bHLH or other proteins were confirmed by performing a BLAST search of the National Center for Biotechnology Information protein sequence database. Polyclonal serum was prepared from whole blood three times after primary and booster immunizations (Beckman Research Institute, Duarte, CA). The specificity of the antibody was tested in Western blots using cell lines with undetectable, low, and high levels of *TWIST* mRNA and by immunohistochemical analysis in tissue sections comparing antibody staining patterns with patterns of *TWIST* message detected by *in situ* hybridization.

Western Blot Analysis

Cells were harvested by scraping into cold PBS and lysed in M-PER protein extraction reagent (Pierce, Rockford, IL) supplemented with protease inhibitors. Nuclear extracts were prepared as previously described [28]. Protein concentrations were determined using the BCA Protein Assay Reagent Kit (Pierce). Proteins were separated in 4% to 15% Tris–HCl gradient polyacrylamide SDS-PAGE gels (Bio-Rad, Hercules, CA) and transferred by electroblotting to an Immun-Blot PVDF membrane (Bio-Rad) in Tris–glycine buffer with 20% methanol. Membranes were blocked with 5% nonfat dry milk (NFDM) in TBST (10 mM Tris, pH 8.0, 150 mM NaCl, and 0.02% Tween-20) for 30 minutes and incubated overnight at 4°C with an antihuman *TWIST* rabbit polyclonal antibody diluted 1:1000 in TBST containing 2% bovine serum albumin (A3059 Fraction V; Sigma). After several washes with TBST, membranes were incubated for 2 hours at room temperature with horseradish peroxidase (HRP)–conjugated goat antirabbit secondary antibodies (Pierce) diluted 1:5000 in TBST containing 3% NFDM. After washes with TBST, antibody binding was visualized on X-OMAT Blue XB-1 film (Kodak, Rochester, NY) by chemiluminescence. For protein loading control, the membranes were stripped and incubated in 5% NFDM/TBST with either anti–β-actin goat polyclonal antibody (Santa Cruz Biotechnology, Santa Cruz, CA), diluted 1:1000 for total proteins, or with INI1 (H-300) rabbit polyclonal antibody (Santa Cruz Biotechnology), diluted 1:400 for nuclear proteins. After washes with TBST, membranes were incubated in 3% NFDM/TBST for 45 minutes with secondary antibodies diluted 1:5000: HRP-conjugated chicken antigoat antibody (Santa Cruz Biotechnology) or HRP-conjugated goat antirabbit antibody (Pierce).

RT-PCR and Southern Blot Analysis

cDNA was synthesized by RT using as a template DNase I–treated total RNA that was extracted from cultured cells and tissues using Trizol (Invitrogen). Controls for genomic DNA contamination were performed without reverse transcriptase on matching samples. The sequences of *TWIST* and *GAPDH* primers and of internal oligonucleotide probes used for Southern blot analysis were either derived from published sources, or designed using the MIT Primer 3 program (Table 1). PCR conditions were optimized to demonstrate linear product formation at the cycle numbers used for *TWIST* detection. Products were identified by Southern hybridization with gene-specific internal oligonucleotide probes. In addition, products from randomly selected RT-PCR reactions for each gene were directly sequenced to confirm their identity. Band density images of Southern hybridizations or ethidium bromide–stained gels were quantified by using Image J shareware (Scion Corporation, Frederick, MD; http://rsb.info.nih.gov/ij/) and normalized to corresponding *GAPDH* readings for the same sample. Band density was determined on a representative Southern hybridization for tumor samples, and in triplicate for mouse astrocyte experiments. Between-group differences were tested for significance by using the Kruskal-Wallis test and *post hoc* Mann–Whitney *U* tests.

In Situ *Hybridization*

Sense and antisense *TWIST* riboprobes were synthesized by *in vitro* transcription from a 298-bp fragment from the 3′UTR of human *TWIST* cloned into pBluescript SK^+ (Stratagene, La Jolla, CA) using T7/T3 polymerases. Twelve-micrometer sections previously fixed in 4% paraformaldehyde were freshly cut from tissue stored at −80°C. *TWIST in situ* hybridization was performed using previously published methods with minor modifications [26] (full protocol available on request). The slides were either washed in water and mounted in aqueous mounting media, or counterstained in methyl green, dehydrated, cleared, and permanently mounted. Adjacent sections were also stained with H&E.

Immunohistochemistry

Tumor or non-neoplastic samples were either fixed fresh frozen with 4% paraformaldehyde or in formalin with paraffin embedding and processed for H&E histology and immunostaining. Frozen samples were fixed in 4% paraformaldehyde, processed for histology, and stored frozen in OCT compound (Sakura Finetek USA, Torrance, CA) at −80°C. Both frozen and formalin-fixed paraffin-embedded samples

Table 1. RT-PCR Primer Sequences and Conditions for Human and Mouse Genes.

	Gene	Forward Sequence	Reverse Sequence	Internal Oligo	T_A	Cycle #	Product Size
Human	*Twist*	GAGTCCGCAGTCTTACGAGG	CTGCCCGTCTGGGAATCACT	TTAGAAGAGCAAAATCCAAA(1) CTACGCCTTCTCGGTCTGGA(2)	59	35	555
	GAPDH	ACGGATTTGGTCGTATTGGG	TGATTTTGGAGGGATCTCGC	ATGGCACCGTCAAGGCTGAG	60	28	231
Mouse	*Twist*	CACGCTGCCCTCGGACAA	GGGACGCGGACATGGACC	GCTGAGCAAGATTCAGACCC	60	30	197
	GAPDH	ATTGTCAGCAATGCATCCTGCA	AGACAACCTGGTCCTCAGTGTA	AACTTTGGCATTGTGGAAGG	59	25	412

were sectioned at 6 μm thickness and processed for antigen retrieval by heating in a microwave oven for 4 minutes at 100% power, then 10 minutes at 10% power in 10 mM citrate buffer, pH 6.0. Sections were allowed to cool to room temperature for 30 minutes before staining. For *TWIST* immunostaining, sections were incubated at 4°C with *TWIST*-specific rabbit polyclonal antibody described above (1:800) with detection of bound primary by the ABC method (Vectastain, Vector Laboratories, Burlingame, CA) using DAB as chromogen. Cell nuclei were visualized by hematoxylin counterstaining. For immunoflourescent detection of TWIST protein in paraffin sections, the same protocol was followed, except that *TWIST* primary antibody was detected with a donkey CY3-conjugated antirabbit IgG (711-165-152, 1:400; Jackson ImmunoResearch Laboratories, West Grove, PA). Double immunofluorescence was performed by sequential staining for TWIST as above, followed by incubation with mouse monoclonal primary antibodies against either NeuN (MAB377, 1:1000; Chemicon, Temecula, CA), GFAP (G3893, 1:500; Sigma), CD45 (M0701, 1:1000; Dako, Carpentiera, CA), or CD68 (M8014, 1:200; Dako), followed by incubation with FITC-conjugated antimouse IgG secondary antibodies (715-095-151, 1:100; Jackson ImmunoResearch Laboratories). Nuclei were counterstained with DAPI (D-1306; Molecular Probes, Eugene, OR), and coverslips were mounted with fluoromount (SouthernBiotech, Birmingham, AL) and light-protected prior to visualization with fluorescent microscopy (Zeiss Axioplan 2, Carl Zeiss USA, Thornwood, NY). Controls omitting primary antibody or using an isotype IgG were performed on all samples. Digitally captured images (Slidebook software; III) were analyzed for double-labeled TWIST immunopositive cells using Image J software (Scion Corporation) by counting at least four ×20 fields from two separate brain samples that included both gray and white matter.

Cell Growth and Saturation Density

For cell growth, 1×10^5 cells in DMEM/F12 supplemented with 10% FBS were plated in 60-mm plates in triplicate. Cells were counted everyday for 4 days using a Coulter counter (Beckman-Coulter, Fullerton, CA). For saturation density assays, 2×10^5 cells were seeded in six-well plates in triplicate. Cells were counted every second day for 7 days.

Matrigel Invasion Assays

The invasion assay was performed using 24-well BD BioCoat Matrigel invasion chambers (BD Biosciences) and QCM cell invasion chambers (Chemicon). Chambers consist of a cell culture insert with an 8-μm pore size membrane coated with a thin layer of BD Matrigel Matrix or Chemicon ECMatrix. SF767 LXSN or SF767Tw cells were harvested, resuspended in a serum-free DMEM, and loaded into the insert (BD Biosciences: 5×10^4 cells/500 μl; Chemicon: 3×10^5 cells/300 μl) according to the manufacturer's recommendations. DMEM/F-12 with 10% FBS was then added to the lower chamber (750 μl for BD Biosciences; 500 μl for Chemicon). Cells were incubated at 37°C for 70 hours (BD Biosciences) or 48 hours (Chemicon) before noninvading cells and matrix gel from the insert were gently removed with a cotton swab. For both assays, invasive cells that penetrated through pores and migrated to the underside of the membrane were stained with the staining solution provided by the manufacturer (Chemicon) for 20 minutes and photographed. For quantitation in both assays, stained cells were dissolved in 200 μl of 10% acetic acid and 100 μl was used for colorimetric reading of OD at 560 nm.

In Vitro *p53-Deficient Model of Astrocyte Transformation*

Mouse astrocytes were cultured from postnatal day 1 mice from wild-type ($p53^{+/+}$), p53 hemizygous ($p53^{+/-}$), or p53 homozygous knockout ($p53^{-/-}$) animals as previously described [22,29]. Frozen cell pellets of $p53^{-/-}$ astrocytes and selected samples of $p53^{+/-}$, $p53^{+/+}$, and $p53^{-/-}$ astrocytes harvested at varying passage numbers were used for the isolation of total RNA and RT-PCR for *TWIST* mRNA.

Results

TWIST *mRNA and Protein Are Frequently Expressed in Glioma Cell Lines*

Examination of rat C6 glioma cells for class B bHLH genes by a degenerate RT-PCR cloning strategy revealed the presence of *TWIST* mRNA. *TWIST* expression in C6 was confirmed by Northern blot analysis (Figure 1*A*), suggesting that *TWIST* may play a role in glial tumorigenesis. To evaluate the relevance of our finding in human gliomas, we examined *TWIST* expression by Northern blot analysis in 11 human cell lines, including six gliomas. Five of six glioma lines expressed variable levels of the documented major 1.4-kb *TWIST* transcript, together with minor transcripts at 2.2 and 3.6 kb (Figure 1*A*) [30,31]. *TWIST* message was also detected in human neuroblastoma and medulloblastoma, but not in colon, breast, or SCLC cell lines examined.

The findings in Northern blot analysis were confirmed and expanded on using RT-PCR to assay *TWIST* expression in a larger panel of 21 human tumor cell lines including those examined by Northern blot analysis. As shown in Figure 1*B*, 11 of 12 glioblastoma (i.e., grade IV) cell lines expressed *TWIST*; RT-PCR confirmed the lack of *TWIST* message revealed by Northern blot analysis of UW455. *TWIST* was also detected by RT-PCR in cell lines derived from neuroblastoma and medulloblastoma—primitive neuroectodermal tumors that arise in the peripheral nervous system and CNS, respectively [32,33]. To our knowledge, this is the first demonstration of *TWIST* expression in medulloblastoma cell lines, whereas expression of *TWIST* in neuroblastoma has recently been described in association with N-myc amplification [12]. As observed in the Northern blot analysis (Figure 1*A*), *TWIST* was not detected in the two colorectal, small cell lung, and breast carcinoma–derived cell lines analyzed by RT-PCR. Our results demonstrate that *TWIST* mRNA is frequently expressed in human glioblastoma–derived cell lines and indicate that *TWIST* expression is a hallmark of glial and nonglial tumors of neuroectodermal lineage.

To analyze TWIST protein in cell lines, first we confirmed the specificity of polyclonal anti-*TWIST* antibody using SF767

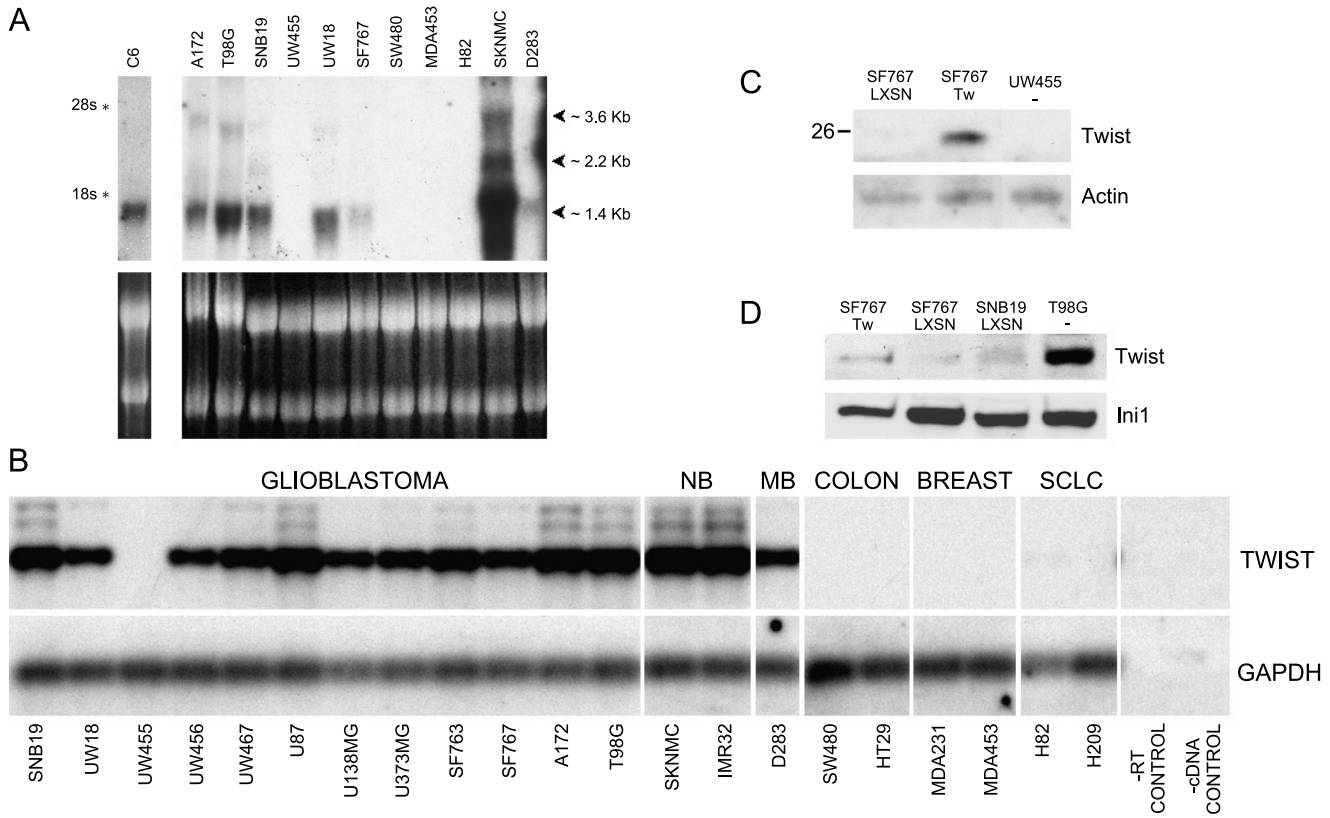

Figure 1. *Expression of* TWIST *mRNA and protein in rodent glioma and human glioblastoma cell lines. (A) Northern blot analysis showing the expression of* TWIST *in rat C6 glioma cells (far left lane), confirming the results of a degenerate RT-PCR screen for class B bHLH genes.* TWIST *mRNA expression was detected in five of six human glioma cell lines (A172, T98G, SNB19, UW455, UW18, and SF767), as well as in lines derived from a neuroblastoma (SKNMC) and a medulloblastoma (D283). Lines derived from colon (SW480), breast (MDA453), and small cell lung cancer (H82) had no detectable expression. The gel stained with ethidium bromide (lower panel) demonstrates equivalent loading and integrity of total RNA. (B) Southern hybridization of* TWIST*-specific probes to RT-PCR products from a larger panel of human tumor cell lines. Blots of* GAPDH *controls show that comparable amounts of total RNA were analyzed for each sample. Differential levels of* TWIST *expression were detected in 11 of 12 human gliomas and in two neuoblastomas and one medulloblastoma, whereas no detectable expression was noted in non-neural tumors.* TWIST *mRNA was not detected by RT-PCR or by Northern blot analysis in the glioblastoma line, UW455, or in the non-neural cell lines examined. (C) Western blot analysis of 30 μg of whole cell lysates of UW455 and SF767, transfected either with an empty expression vector (LXSN) or a* TWIST *overexpression construct (Tw), demonstrates the presence of a band at the expected molecular mass of 26 kDa. UW455, which lacks detectable* TWIST *mRNA and SF767LXSN with low basal message levels, shows no detectable protein. (D) Nuclear extracts of the SF767LXSN, SNB19LXSN, and T98G cell lines (50 μg each) demonstrate endogenous expression of a 26-kDa TWIST protein comparable to that detected in nuclear extracts from SF767Tw (10 μg) at levels commensurate with mRNA levels (panel A). The nuclear protein, INI1, is used to compare the levels of nuclear-specific protein loaded from each preparation.*

cells transduced with *TWIST*-expressing retrovirus. We chose SF767 cells because they express low basal levels of message by Northern blot analysis (Figure 1*A*). UW455 cells, which lack detectable *TWIST* message (Figure 1*A*), served as a negative control. Figure 1*C* shows that in 30 μg of whole cell extracts of glioma cells overexpressing *TWIST* (SF767Tw), the antibody detected a single protein band of approximately 26 kDa. The 26-kDa molecular weight is consistent with the previously reported size for the TWIST protein [30]. Then we tested endogenous levels of *TWIST* expression in glioblastoma cell lines using cell nuclear extracts. Because endogenous levels of TWIST protein are low, we reduced the amount of nuclear proteins from positive control cells (SF767Tw) loaded on the gel to 10 μg, whereas 50 μg of nuclear extracts from other cell lines was loaded alongside (Figure 1*D*). Levels of endogenous TWIST protein of the same molecular weight were detected and correlated well with Northern blot analysis of RNA from the same cell lines. Therefore, we conclude that the polyclonal *TWIST* antibody interacts specifically with TWIST protein, and that TWIST protein present in human glioma cell lines reflects steady-state levels of *TWIST* mRNA.

TWIST *mRNA Content Is Associated with Grade in Human Gliomas*

We examined 10 grade II, 6 grade III, and 12 grade IV gliomas of differing histologies to determine if *TWIST* mRNA is expressed *in vivo* in human gliomas. Nineteen tumors were newly operated, whereas nine had recurred after either previous surgery (n = 1), surgery followed by radiotherapy (n = 3), or surgery followed by radiotherapy and chemotherapy (n = 5). Using semiquantitative RT-PCR, *TWIST* mRNA was detected in 89% (25 of 28) of gliomas (Figure 2, *A* and *B*). *TWIST* abundance did not differ discernibly between newly operated and recurrent tumors (Figure 2*A*). As shown in Figure 2, *B* and *C*, mean *TWIST* transcript band

intensity, expressed as a percentage of that for *GAPDH*, was approximately three-fold greater in grade IV than in grade II tumors (29.6 ± 24.5 *vs* 10.0 ± 8.9; $P = .015$) and in combined grade II and III tumors (10.5 ± 7.4; $P = .01$). Mean normalized *TWIST* expression in grade III gliomas (11.2 ± 4.5) was markedly less than grade IV, but the difference was not statistically significant ($P = .09$). These results indicate that overall *TWIST* mRNA levels reflect degree of malignancy (Figure 2*C*), a conclusion supported by the observation that the three tumors with no detectable *TWIST* were grade II. Nonetheless, *TWIST* levels varied considerably between and within diagnostic subtypes, as evidenced by the ~70-fold range of normalized *TWIST* content for grade IV (Figure 2*B*). Our data indicate that *TWIST* mRNA expression commonly accompanies glial tumorigenesis, and that higher expression is associated with grade IV tumors.

TWIST *Expression Is Localized to Tumor Cells*

To elucidate the intratumoral localization of *TWIST* mRNA in gliomas, we examined expression by *in situ* hybridization in two grade II, one grade III, and three grade IV gliomas; representative results are shown in Figure 3. Importantly, *TWIST*-specific hybridization reflected *TWIST* mRNA content detected by RT-PCR as evidenced by greater hybridization associated with increasing tumor grade. Thus, a low-grade glioma with barely detectable *TWIST* expression by RT-PCR (sample 7; Figure 2*A*) showed only faintly discernible hybridization (Figure 3*E*), whereas two grade IV gliomas with high levels of *TWIST* mRNA (samples 24 and 28 in Figure 2*A*) showed intense hybridization in a majority of cells (Figure 3, *F* and *G*). Notably, the grade IV tumors displayed *in situ* hybridization signal intensity comparable to that of rhabdomyosarcoma (Figure 3*H*), a highly malignant mesenchymal neoplasm known to overexpress *TWIST* [10]. Although the overall intensity of *TWIST* hybridization corresponded to tumor grade, hybridization intensity varied markedly among cells within a glioma (Figure 3, *E*–*H*). The variation in *TWIST* message abundance in these samples was corroborated by immunostaining of the same specimens (Figure 3, *I*–*L*). Although only sparse immunoreactivity was detected in the low-grade tumor (Figure 3*I*), markedly elevated TWIST immunoreactivity was demonstrated in tumor nuclei of samples from the grade IV gliomas (Figure 3, *J* and *K*) and rhabdomyosarcomas (Figure 3*L*).

TWIST *Expression and Malignant Progression*

The increased levels of mRNA expression in grade IV tumors suggest that elevation of *TWIST* accompanies the malignant progression of gliomas. To further characterize the association of *TWIST* with malignant progression in gliomas, we examined changes in mRNA and protein content that accompanied the recurrence of a low-grade oligodendroglioma as a grade IV glioblastoma in the same patient. As shown in Figure 4, TWIST protein content detected by immunostaining (Figure 4, *A* and *B*) and *TWIST* mRNA abundance (Figure 4*D*) was markedly increased in the high-grade recurrence. Importantly, the increase in TWIST protein content colocalized with malignant histologic hallmarks (increased cellularity, nuclear and cellular atypia, endothelial proliferation, and necrosis) in the recurrent tumor (Figure 4*C*).

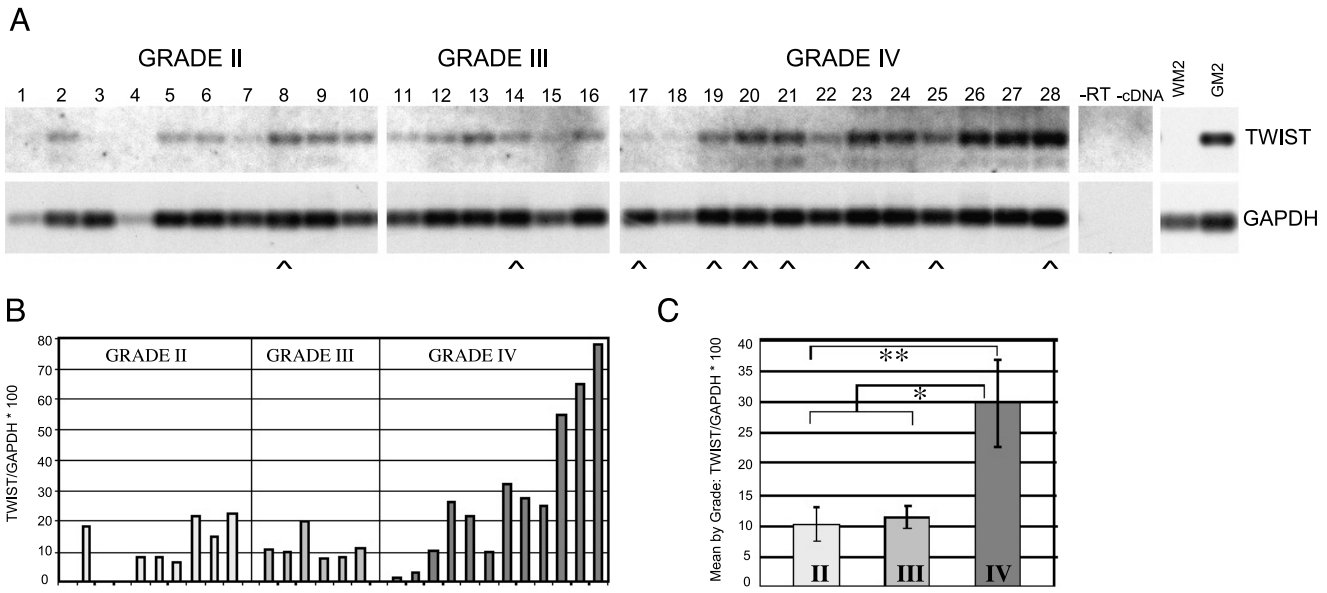

Figure 2. *TWIST expression in human gliomas. The abundance of mRNA was analyzed by Southern hybridization of* TWIST- *and* GAPDH-*specific probes to RT-PCR products. (A) Glial tumors, grouped by grade, include grade II fibrillary astrocytomas (1–3), oligodendroglioma (4–9), and mixed oligoastrocytoma (10); grade III anaplastic mixed oligoastrocytomas (11–13) and anaplastic astrocytoma (14–16); and grade IV glioblastoma (17–26) and gliosarcoma (27 and 28). The nine tumors recurrent after prior treatment are indicated by a caret beneath the corresponding lane. No statistical difference in gene expression levels between primary or recurrent samples was noted (data not shown). Representative RT-PCR controls without RT or cDNA are shown at the far right. (B) Histogram of relative* TWIST *expression for gliomas, grouped by grade. The signal density of* TWIST *is expressed as a percentage of the corresponding* GAPDH *signal. (C) Mean relative* TWIST *expression with standard errors of the mean by glioma grade. Significant differences ($P \leq .05$) indicated by asterisks were demonstrated between grades II and IV (**) and combined grade II plus grade III and IV tumors (*).*

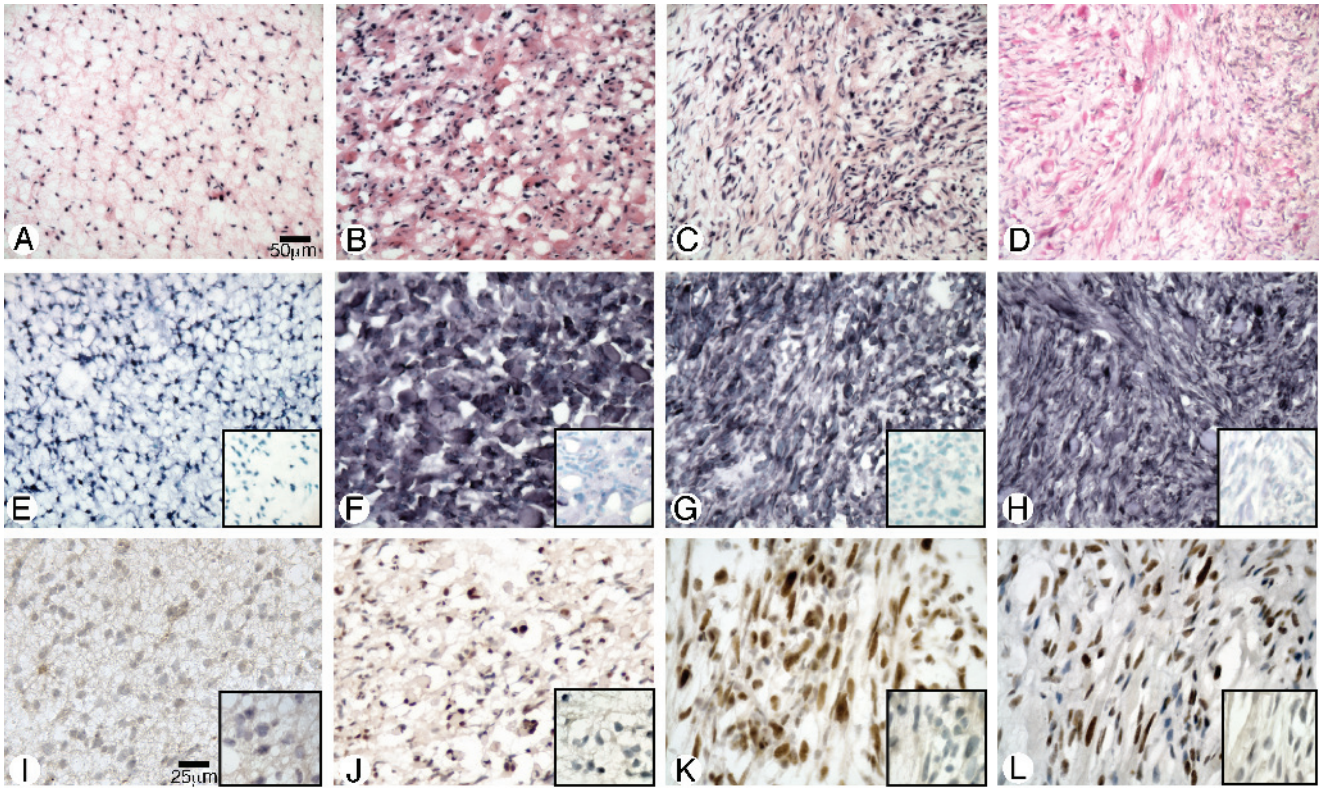

Figure 3. TWIST *expression patterns in low-grade and high-grade gliomas by* in situ *hybridization and immunostaining. H&E histology (A–D),* TWIST in situ *hybridization (E–H), and immunostaining (I–L) are shown from adjacent sections of sample 7, a grade II glioma with low levels of* TWIST *by RT-PCR (A, E, and I); sample 24, a grade IV glioblastoma (B, F, and J); sample 28, a grade IV gliosarcoma (C, G, and K) with strong* TWIST *expression; and a rhabdomyosarcoma (D, H, and L), previously reported to express* TWIST *[10]. H&E and* in situ *hybridization photomicrographs were taken with* ×*20 objective, whereas iummunostained images were taken with a* ×*40 objective. Sense control hybridization reactions for each sample are shown as insets in the right lower hand corner (E–H).* In situ *hybridization sections were counterstained with methyl green to facilitate visualization of tissue architecture. Immunostaining demonstrates occasional faint staining in the low-grade sample (I), whereas abundant pronounced nuclear staining is present in all of the high-grade tumors (J–L). Nuclear staining is not apparent in isotype IHC controls (lower right corner insets), indicating the specificity of the antibody. (The 50-*μ*m scale bar in (A) applies to (A)–(H), and the 25-*μ*m scale bar in (I) applies to (I)–(L).)*

Areas histologically similar to the original low-grade glioma either lacked or exhibited low levels of TWIST protein (data not shown). This correlation between the presence of *TWIST* and anaplastic histologic features suggests that, in this case, elevated levels of TWIST protein expression accompanied malignant glial progression. This observation supports a role for *TWIST* in malignant progression.

Elevation of TWIST *mRNA Precedes* In Vitro *Transformation of Mouse Astrocytes*

To gain additional insights into the association of *TWIST* with glial tumorigenesis, we analyzed its expression in an *in vitro* model of astrocyte transformation. Cultured neonatal mouse astrocytes hemizygous for p53 spontaneously undergo a well-defined sequence of genetic and physiological changes culminating in malignant transformation [22–34]. We examined by RT-PCR the abundance of *TWIST* mRNA in serially passaged $p53^{+/-}$ mouse astrocytes derived from postnatal day 1 animals. As shown in Figure 5, *TWIST* mRNA content normalized to GAPDH was approximately 10- and 7-fold greater in $p53^{+/-}$ than in $p53^{+/+}$ cells at passages 1 and 4, respectively. By passage 8, when these cells are known to lose the remaining wild-type copy of p53 and develop aneuploidy [22], *TWIST* expression increased an additional 30%. Similar changes in *TWIST* expression were observed in homozygous $p53^{-/-}$ astrocytes (data not shown). *TWIST* content remained elevated through passage 50, at which time the cells displayed serum-independent growth and formed tumors *in vivo* [22]. In contrast, *TWIST* abundance was unchanged in wild-type astrocytes through passage 4, the approximate limit of their proliferative potential *in vitro*, and was comparable to the level in adult wild-type mouse brain. Wild-type astrocytes senesce by passage 6 or 7 and additional comparison of *TWIST* levels with p53-deficient astrocytes at subsequent serial passage numbers are not possible. Our data suggest that elevated *TWIST* expression accompanies loss of p53 function and the resulting increase in genomic instability associated with malignant transformation.

Overexpression of TWIST *Promotes Glioma Cell Invasion*

To delineate potential roles for *TWIST* in glioma biology, we examined the effect of *TWIST* overexpression in SF767 (SF767Tw) on cell proliferation, saturation density, and invasion through an artificial basement membrane matrix. As shown in Figure 6*A*, SF767Tw cells displayed slightly slower

growth rates that led to reduced saturation density (Figure 6*B*) compared to SF767 containing vector alone. Interestingly, suppression of *TWIST* expression in 4T1 mouse mammary carcinoma cells resulted in a small increase in growth rate [15]. *TWIST* overexpression has been reported to alter cell morphology in MDCK kidney epithelial cells, immortalized human mammary epithelial cells [15], and osteosarcoma cells [30], but similar morphologic changes in *TWIST*-overexpressing SF767 cells were not observed (data not shown). The report that *TWIST* expression is necessary for mammary carcinoma metastasis in rodents and is elevated in invasive human breast-carcinomas led us to hypothesize that *TWIST* promotes invasion by human gliomas. In accord with our hypothesis, SF767Tw displayed greater infiltration through two different Matrigel extracellular matrices than control cells (Figure 6, *C and D*). These findings suggest that, by promoting invasiveness, *TWIST* contributes to a hallmark characteristic of human gliomas.

TWIST *Is Expressed in Normal Fetal and Adult Human Brain*

Expression of *TWIST* in developing or adult mammalian brain has not been unambiguously delineated [31,35]. To better clarify the potential role of *TWIST* expression in gliomagenesis, we examined *TWIST* mRNA content in human developing and mature brain by RT-PCR. As shown in Figure 7*A*, abundant levels of *TWIST* were detected in all samples of embryonic and fetal brain that ranged from day 52/53 to day 132 postconception, suggesting that *TWIST* participates early in the development of the human brain. Notably, the level of expression in developing brain was comparable to that in mesenchyme-derived human embryonic bone (Figure 7*A*). *TWIST* was also detected by RT-PCR at levels comparable to that of adult temporalis muscle in seven non-neoplastic brain samples obtained from adults operated either for epilepsy (four males and one female, 36–46 years old) or benign skull base tumors (two males, 32 and 48 years old). *TWIST* message was detected by *in situ* hybridization (data not shown) in adult muscle in satellite cells, consistent with previous observations that *TWIST* is expressed in adult myoblasts [36]. In brain samples that were macroscopically dissected from fresh brain tissue, *TWIST* expression was exclusively detected in the gray matter in three of four specimens with only trace expression in one of four white matter specimens. Representative results are shown in Figure 7*A*. *In situ* hybridization performed on two brain specimens corroborated these findings and revealed pronounced staining of cells with morphologic characteristics of neurons (Figure 7, *B* and *C*), with rare staining evident in white matter, which did not localize to morphologically identifiable cell types (Figure 7, *F* and *G*). Immunostaining of normal gray matter (Figure 7*D*) and white matter (Figure 7*H*) or gray–white junction (Figure 7, *E* and *I*) samples further corroborated the findings of RT-PCR and *in situ* hybridization, which

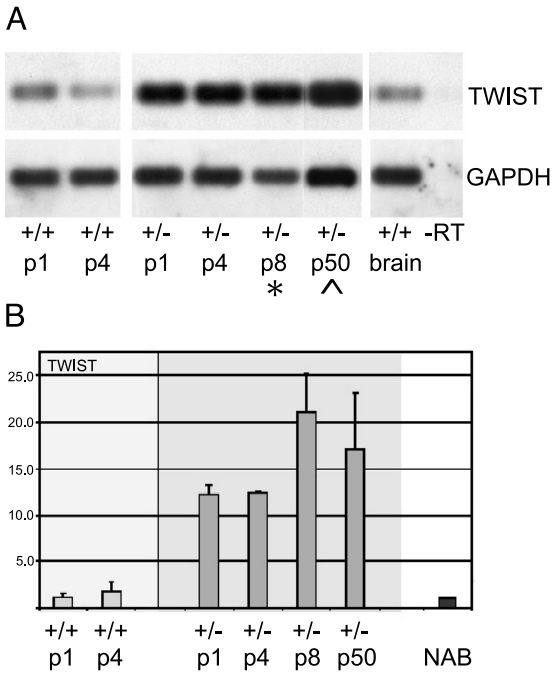

Figure 5. TWIST *mRNA abundance is elevated by p53 deficiency in mouse astrocytes. (A) Comparison of* TWIST *mRNA detected by Southern hybridization of RT-PCR reaction products from cultured p53 wild-type (+/+) and hemizygous (+/–) astrocyte cultures derived from neonatal mice. Also shown are levels in normal adult mouse brain (NAB) and a control lacking RT. (B) Density of* TWIST *mRNA signal normalized to that of* GAPDH *of samples shown in (A). Values are the mean ± SD of three independent determinations. The appearance of features accompanying malignant transformation at specific passage numbers is indicated as follows: DNA ploidy abnormalities (*), serum-independent growth, and tumor formation in nude mice (^). The marked increase of* TWIST *expression in p53$^{+/-}$ astrocytes relative to normal brain and wild-type astrocytes at passages 1 and 4 is maintained through serial passages coinciding with progressive acquisition of malignant phenotype* in vitro*, including complete malignant transformation (growth of solid tumors* in vivo*) by passage 50.*

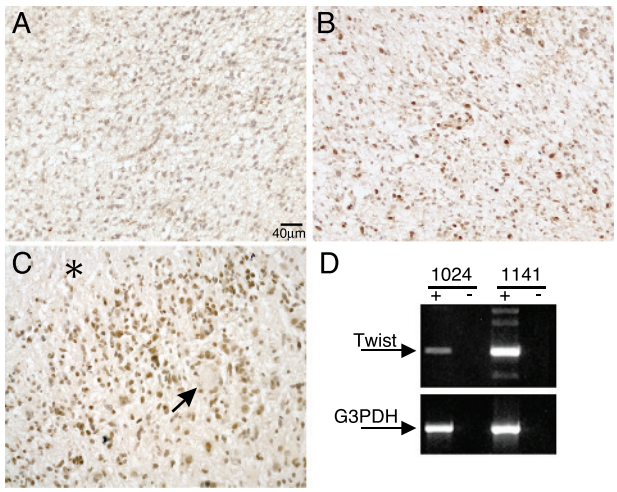

Figure 4. *Increased TWIST protein and mRNA content accompanies malignant progression. Immunostaining revealed increased abundance of TWIST protein accompanying the recurrence of a grade II oligodendroglioma (A) to a grade IV glioblastoma (B). The recurrent tumor demonstrates increased cellularity characteristic of glioblastoma, together with pronounced TWIST immunopositivity in tumor cell nuclei. High levels of TWIST protein (C) were particularly evident in areas of the recurrent tumor with malignant histologic features of increased cellularity, necrosis (asterisk), and microvascular proliferation (arrow). In accord with the elevated level of TWIST protein evident by immunostaining, the recurrent sample demonstrates increased abundance of TWIST mRNA by RT-PCR (D). (The 40-μm scale bar in (A) applies to (A)–(C).)*

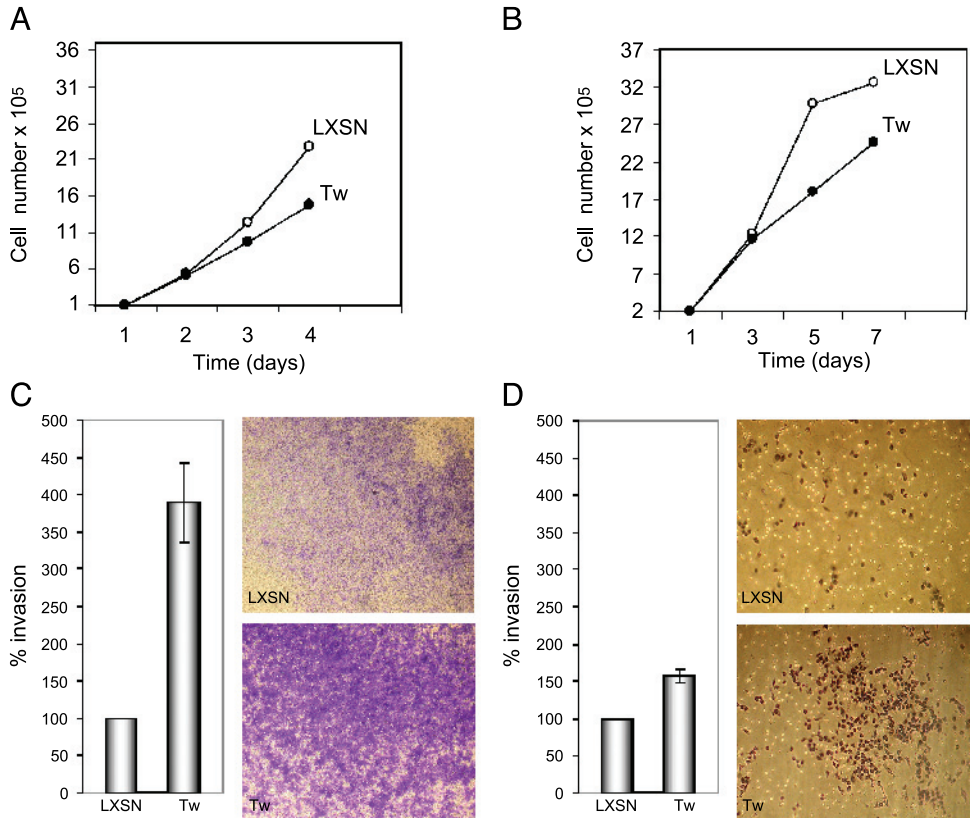

Figure 6. *Overexpression of* TWIST *promotes invasion but not cell proliferation in SF767 glioma cells. (A) The impact of* TWIST *overexpression on cell growth rate in culture was examined by plating 1 × 10⁵ SF767Tw or SF767 LXSN vector control cells in 60-mm plates in triplicate. Cells were trypsinized and counted each day for 4 days using a Coulter counter, and the mean of three wells from each time point is shown. (B) TWIST effects on cell saturation density were assayed by plating 2 × 10⁵ SF767Tw or SF767 LXSN vector control cells in six-well plates in triplicate. Triplicate wells were trypsinized and counted every second day for 7 days using a Coulter counter and plotted. Calculated standard errors were small and cannot be visualized at this scale. (C, D) Invasion through two extracellular matrices is increased by overexpression of* TWIST *in SF767 assayed by two separate invasion assays (C, Chemicon; D, BD Biosciences). Data were analyzed after 70 hours for BD Biosciences and 48 hours for the Chemicon assay. Photomicrographs of stained cells on the undersurface of matrix-coated 8-μm pore size filter demonstrate differential invasion of SF767 LXSN and SF767 TW cells. Cells from triplicate assays were stained and quantified by colorimetric reading at OD of 560 nm. Invasion by SF767TW was calculated as a percentage of the SF767 LXSN vector control values. Data shown are mean ± SE.*

suggested that in normal brain, TWIST protein and mRNA are almost exclusively localized to neurons in gray matter.

TWIST *Expression in Adult Brain Localizes to Neurons*

The identity of *TWIST*-expressing cells in the normal brain is of central importance to establishing the importance of *TWIST* in human gliomagenesis. To confirm the results of *in situ* hybridization, which suggested that *TWIST* mRNA expression is confined to neurons, we performed double-label immunofluorescent staining experiments using two different normal brain samples and found that of 315 *TWIST*-expressing cells, 305 (or 97%) coexpressed the neuronal marker NeuN (Figure 8, *A–C*). Conversely, we were not able to unambiguously identify any *TWIST*-expressing cells that coexpressed GFAP (Figure 8, *D–F*), indicating that TWIST protein expression is almost exclusively restricted to neuronal cells in the non-neoplastic human brain. TWIST protein was not detectable in white matter (Figures 7, *H* and *I* and 8*F*), in agreement with *in situ* hybridization and RT-PCR results. Our analysis also indicated that *TWIST* is not expressed in lymphocytes or microglia (data not shown). To our knowledge, these results are the first evidence of expression of *TWIST* mRNA and protein in human developing brain and mature neurons. Our findings suggest that *TWIST* participates in the development of the CNS, and may have as yet undetermined roles in the biology of mature neurons. The restriction of expression to neurons indicates that *TWIST* in human glioma cells is a consequence of oncogenic transformation, rather than persistent expression of a gene present in normal glia.

Discussion

Primary brain tumors remain among the most lethal of human cancers despite more than three decades of intensive effort to develop more effective surgical techniques, and radiation-based and chemotherapy-based adjuvant therapies [37,38]. The persistent dismal prognosis for the most common brain malignancies in adults and children has stimulated the search for novel therapies. The recognition that neural precursor cells in the adult brain are the likely targets for malignant transformation [39–41] has stimulated

investigation of the recapitulation of developmental gene expression during glial tumorigenesis in the hope of uncovering new targets for therapeutic intervention. Here we show that human gliomas frequently express *TWIST*, an essential regulator of mesodermal development [42]. Expression was observed in all major glioma diagnoses as well as in medulloblastoma-derived and neuroblastoma-derived cell lines, indicating that *TWIST* participates in the genesis of a wide range of neuroectodermal tumors. Expression was also observed in embryonic and fetal brain and, unexpectedly, in mature neurons, suggesting that *TWIST* promotes gliomagenesis by the aberrant activation of a previously unrecognized pathway(s) normally involved in the development and function of the human CNS. Importantly, the demonstration that *TWIST* promotes glioma cell invasion supports functions for *TWIST* in human gliomas similar to those demonstrated for other non-neural cancers [15].

Current evidence indicates that *TWIST* functions as an oncogene by enhancing cell survival through inhibition of p53-mediated apoptosis [10], preventing growth arrest that accompanies developmental maturation [36,43–46] and promotion of tumor cell invasiveness [15]. The ability of *TWIST* to foster cell survival would enhance tumor progression by increasing resistance to cytotoxic therapies as well as endogenous cytotoxic stresses such as reactive oxygen free radicals generated in association with increased cellular proliferation [47,48]. Indeed, elevated levels of *TWIST* in other transformed or normal cells are associated with resistance or reduced sensitivity to cytotoxic drugs [14,35]. The antiapoptotic function of *TWIST* may be a primary defense against endogenous insults in the sizeable minority of gliomas that possess functional p53 and may also provide a secondary or complementary mechanism that promotes survival in the majority of gliomas in which p53 function is

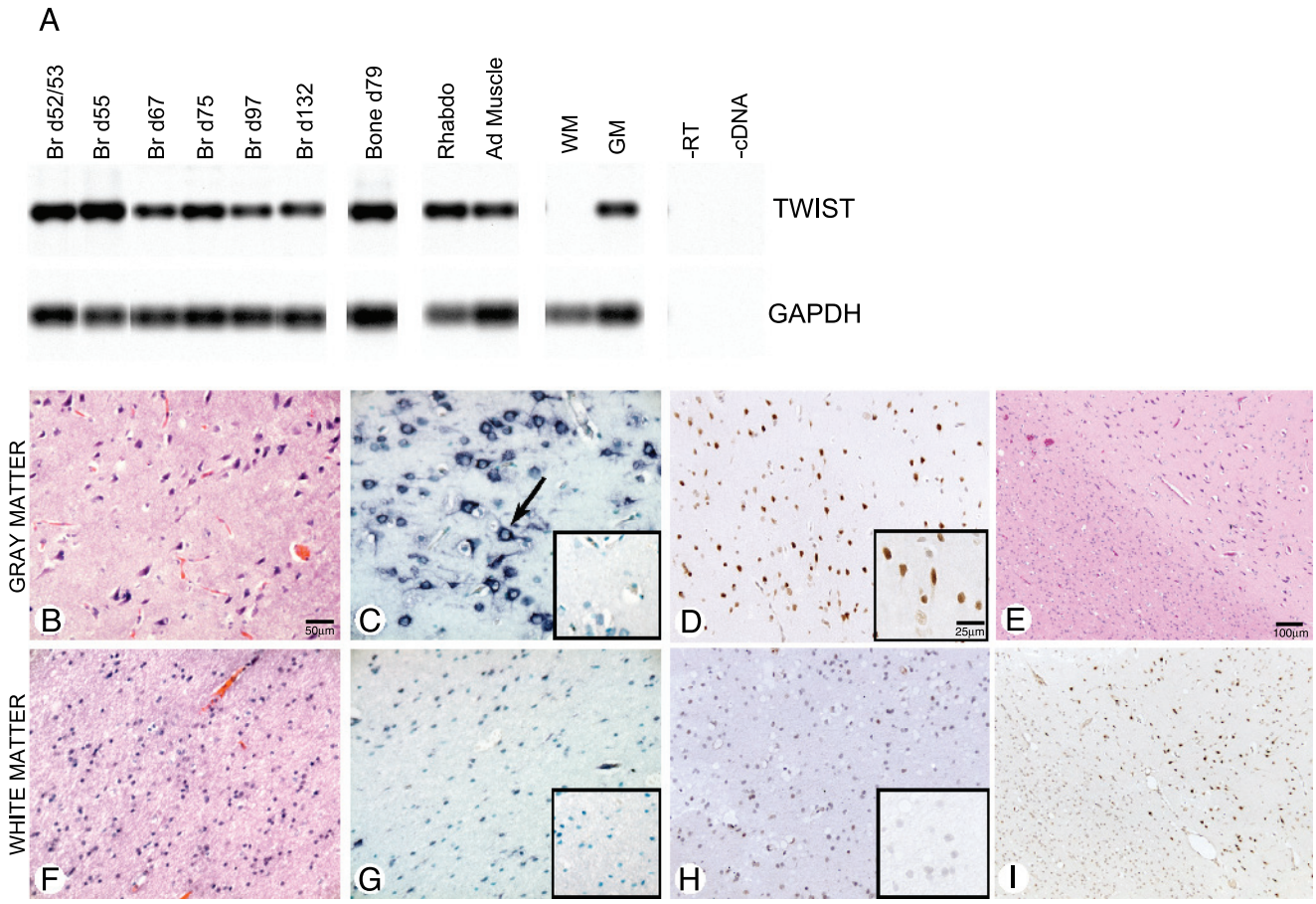

Figure 7. *Expression of* TWIST *in human developing and adult brain. (A) Southern hybridization of RT-PCR reactions from embryonic, fetal, and adult tissues including control bone tissue (79 days) known to express* TWIST *and a panel of embryonic and fetal brain (Br) samples from 52/3 to 132 days showing* TWIST *expression throughout this developmental time frame.* TWIST *expression in temporalis muscle (Ad Muscle) and rhabdomyosarcoma (Rhabdo) is consistent with the known expression of* TWIST *in adult muscle progenitor cells [36] and the mesenchymal-derived tumor [10].* TWIST *is differentially expressed in adult brain, with expression detected in gray matter (GM) but at low or undetectable levels in white matter (WM). (B and F) H&E histologic sections (×20) of normal gray matter (B) and white matter (F) are compared with ISH (×20) for* TWIST *expression from adjacent sections of gray (C) and white matter (G). Insets in the right lower corner (C and G) are sense controls.* TWIST *IHC (×20) for normal gray matter (D) and white (H) matter corresponds to expression patterns by ISH. Inset: ×40 images in (D) and (H) demonstrate nuclear staining pattern in cells with neuronal morphology. (E and I) The demarcation of TWIST protein expression between normal gray and white matter is demonstrated in low-power (×10) photomicrographs of a normal brain sample with a diagonally oriented junction between gray (upper right) and white matter (lower left) by H&E histology (E) and* TWIST *IHC (I). These data indicate that* TWIST *message and protein are almost exclusively detected in gray matter. (The 50-μm scale bar in (B) applies to (B)–(D) and (F)–(H); the 25-μm scale bar in the (D) inset applies to insets of (D) and (H); and the 100-μm scale bar in (E) applies to (E) and (I).)*

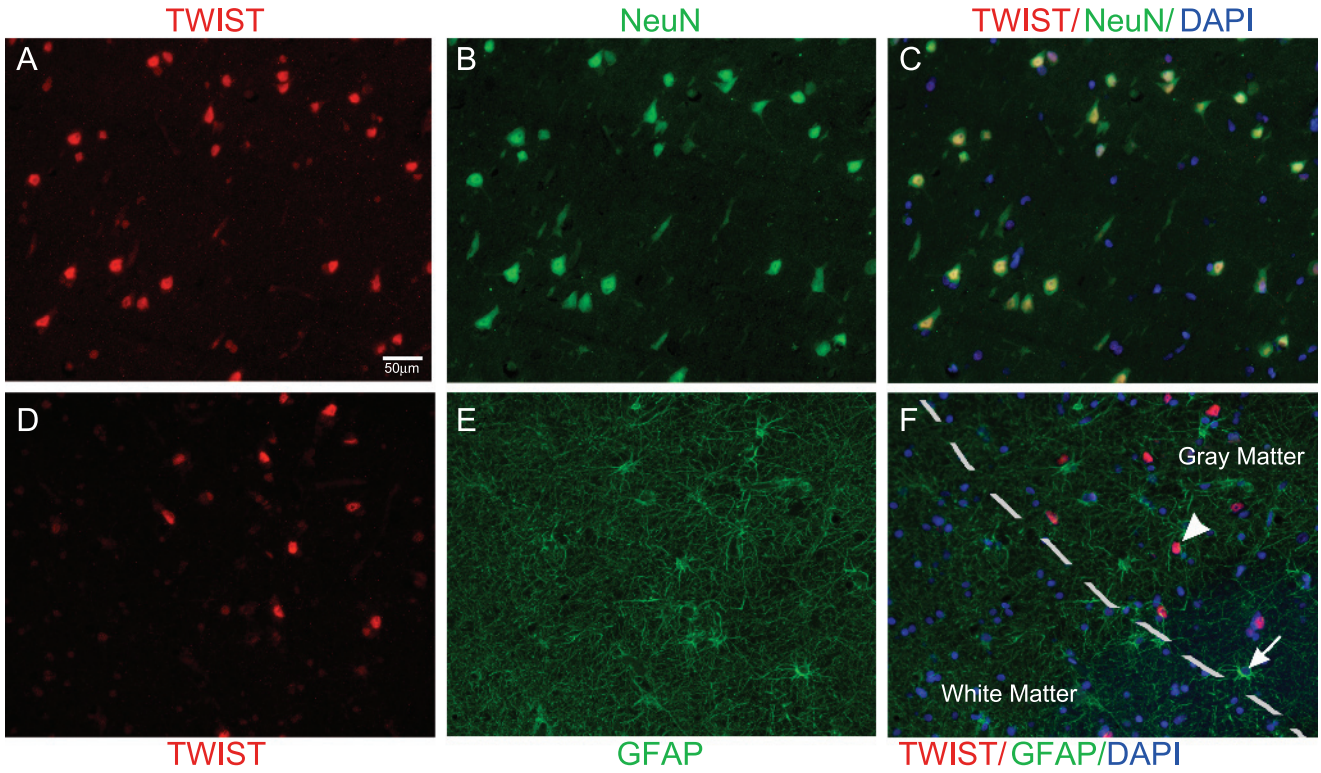

Figure 8. TWIST *is expressed almost exclusively in neurons of the adult brain. (A–C) Photomicrographs of indirect immunofluorescent staining with* TWIST *antibody (Cy3) of normal human gray matter (A), the neuronal marker NeuN (FITC) (B), and the merged image (C) show colocalization of* TWIST *with NeuN in almost every* TWIST *immunoreactive cell (arrow). Sections were also stained with DAPI and indicate that NeuN-negative cells do not express* TWIST. *(D–F) A section of normal human brain containing gray and white matter stained for* TWIST *(Cy3) (D) and GFAP (FITC) (E), and the merged image with DAPI nuclear stain (F) demonstrate that* TWIST *is found exclusively in gray matter and that* TWIST*-expressing nuclei (arrowhead) do not colocalize with GFAP-immunopositive cells (arrow). The junction between gray and white matter is indicated by the dotted line. These results demonstrate that* TWIST *is almost exclusively found in neurons. (The 50-μm scale bar in (A) applies to (A)–(F).)*

suppressed or inactivated [49–51]. In accord with this hypothesis is the observation that coexpression of c-*myc* and *TWIST* inhibits p53-mediated apoptosis and promotes transformation in embryonic mouse fibroblasts [10].

Recently, it has been shown in neuroblastoma that oncogenic cooperation between *TWIST* and N-myc promotes malignant transformation and cell survival in response to cytotoxic stress by inhibiting p53 function [12]. In genetically engineered mice, c-*myc* overexpression targeted to GFAP-expressing cells produces tumors analogous to human glioblastoma [52]. Notably, grade III and IV human gliomas demonstrate marked elevations of c-*myc* expression relative to normal brain and low-grade tumors [53]. Thus, these data and our demonstration of *TWIST* mRNA and protein in human gliomas suggest that, similar to neuroblastoma, oncogenic cooperation between *TWIST* and other oncogenes such as c-*myc* may contribute to glioma treatment resistance by promoting cell survival, in part, through abrogation of p53-mediated apoptosis.

Another function of *TWIST* relevant to human gliomas is promotion of EMT. In epithelial-derived solid tumors, EMT is a critical component of the metastatic cascade whereby transformed epithelial cells lose normal cell–cell interaction and adopt a mesenchymal phenotype characterized by invasion through basement membrane [54]. *TWIST* expression has been associated with EMT in gastric carcinoma [13] and is essential in mouse mammary carcinoma models for EMT and metastasis, in part, by promoting cell motility [15]. Of note, elevated levels of *TWIST* are found in the most invasive types of breast carcinoma cell lines and tumors [15]. In the present study, the highest levels of *TWIST* expression were present in grade IV tumors and overexpression of *TWIST* promoted glioma invasion *in vitro*. Tumor cell migration and invasion into surrounding brain are two features of human gliomas that increase with tumor grade. Thus, the promotion of invasion appears to be a function of *TWIST* shared by both breast and glial cancers. The limitations to surgical resection and effective delivery of systemic and local therapies posed by the diffusely invasive behavior of glioma tumor cells underscore the importance of characterizing *TWIST* function in primary brain tumors.

Although direct evidence is currently lacking, *TWIST* function may also be linked to the activation of receptor tyrosine kinases (RTKs) overexpressed in human gliomas that control cell survival and invasion. In other cell types, *TWIST* expression is elevated by the RTKs IGFR1 and c-met, whose ligands are IGF-1 and HGF, respectively [35,36]. Antisense-mediated suppression of *TWIST* reduces the ability of IGF-1 to rescue NIH 3T3 fibroblasts from etoposide-mediated cell death [35]. In human gliomas, both RTKs are overexpressed

and their signaling pathways are activated, in direct correlation with tumor grade [35,55–58]. Importantly, activation of the IGF-1/IGFR1 and HGF/c-met signaling pathways promotes survival of glioma cells exposed to cytotoxic agents [58–60] and enhances tumor cell migration and invasiveness [61–64]. Of particular interest, IGF-1/IGFR1 and HGF/c-met signaling activates AKT [58,65], which mediates increased resistance to apoptosis demonstrated by migratory glioma cells [66]. These observations and the demonstrated role for *TWIST* in regulating glioma cell invasion and survival in other cancers warrant further investigation of *TWIST* interactions with RTK signaling and activation of AKT.

Our examination of embryonic, fetal, and mature human brain, the most comprehensive to date, unambiguously indicates that *TWIST* expression is associated with early development of the human CNS. Conceivably, the antiapoptotic and invasion-promoting activities of *TWIST* facilitate the migration and expansion of neural progenitor populations during CNS development. We note that our findings stand in contrast to an earlier report of an absence of *TWIST* in human fetal astrocytes and adult human brain by Northern blot analysis [31]. Our analyses, however, support the expression of *TWIST* in fetal brain, and in neurons in adult brain. The low levels of *TWIST* expression detected in mouse neonatal astrocytes and adult human white matter, and the relative differences in sensitivity between Northern blot analysis and RT-PCR analysis may account for these differences. *TWIST* promotes resistance to p53-mediated apoptosis and cell proliferation, and inhibits differentiation in experimental models [10,46]. Accordingly, in normal tissues, its expression has predominately been localized to proliferative and immature cells of mesodermal origin [67–69], although expression in some mature cell types has been described [31,67]. Thus, finding *TWIST* mRNA in mature neurons was unexpected. It is conceivable that the antiapoptotic function of *TWIST* operates in quiescent neurons as well as in proliferating cells. Neuronal activity is associated with high rates of oxygen utilization that elevate the rate of endogenous generation of reactive oxygen free radicals. *TWIST* would likely promote neuronal survival by inhibiting the induction of apoptosis by these damaging agents.

Our results, together with previous findings in other human tumors, suggest the following model in which *TWIST*, by promoting survival, malignant progression, and invasion, facilitates glial tumorigenesis and glioma clinical behavior. *TWIST* in low-grade gliomas may promote resistance to endogenous and exogenous cytotoxic stress that would otherwise lead to apoptotic cell death. By promoting survival, *TWIST* could facilitate the accumulation and propagation of mutations that are associated with glial tumor progression. *TWIST* could then interact synergistically with mutation-induced oncogene activation, in similar fashion to the oncogenic cooperation observed between N-myc and *TWIST* in neuroblastoma [12], to promote and maintain a more malignant phenotype. Candidate target oncogenes for interaction with *TWIST* include RTKs as well as c-*myc*. This scenario outlines the potential functions of *TWIST* related to the genesis of low-grade gliomas and their malignant progression to "secondary" glioblastomas. In the case of "primary" glioblastoma, which infrequently demonstrates p53 mutations [70], *TWIST* may function alone or in combination with other oncogenes to promote tumor growth and treatment resistance, in part by inhibiting p53-mediated apoptosis. Importantly, *TWIST* may promote glioma cell invasion of surrounding normal brain, a major factor contributing to the dismal prognosis for glial tumors. The mechanisms by which *TWIST* contributes to gliomagenesis and glioma physiology and normal CNS development remain to be more fully characterized. Elucidating the pathways that elicit aberrant *TWIST* expression in gliomas, as well as characterizing the effectors of *TWIST* activity, are likely to provide new insights into the genesis of gliomas and to identify new targets for therapeutic intervention.

Acknowledgements

We thank Janet Schukar and Paul Schwartz for their assistance with figure preparation; Rosemary Kimmel for editorial assistance; Alan Fantel (Birth Defects Research Laboratory, Department of Pediatrics, UW) for provision of human fetal tissues; Carol Fahrenbruch for assistance with statistical analysis; and Stephen Kendall, PhD (City of Hope), for assistance with antibody characterization.

References

[1] Weintraub H, Davis R, Tapscott S, Thayer M, Krause M, Benezra R, Blackwell TK, Turner D, Rupp R, Hollenberg S, et al. (1991). The *myoD* gene family: nodal point during specification of the muscle cell lineage. *Science* **251** (4995), 761–766.

[2] Doyle K, Zhang Y, Baer R, and Bina M (1994). Distinguishable patterns of protein–DNA interactions involving complexes of basic helix–loop–helix proteins. *J Biol Chem* **269** (16), 12099–12105.

[3] Chen ZF and Behringer RR (1995). Twist is required in head mesenchyme for cranial neural tube morphogenesis. *Genes Dev* **9** (6), 686–699.

[4] Soo K, O'Rourke MP, Khoo PL, Steiner KA, Wong N, Behringer RR, and Tam PP (2002). Twist function is required for the morphogenesis of the cephalic neural tube and the differentiation of the cranial neural crest cells in the mouse embryo. *Dev Biol* **247** (2), 251–270.

[5] Zuniga A, Quillet R, Perrin-Schmitt F, and Zeller R (2002). Mouse Twist is required for fibroblast growth factor–mediated epithelial–mesenchymal signalling and cell survival during limb morphogenesis. *Mech Dev* **114** (1–2), 51–59.

[6] Li L, Cserjesi P, and Olson EN (1995). Dermo-1: a novel twist-related bHLH protein expressed in the developing dermis. *Dev Biol* **172** (1), 280–292.

[7] Hebrok M, Fuchtbauer A, and Fuchtbauer EM (1997). Repression of muscle-specific gene activation by the murine Twist protein. *Exp Cell Res* **232** (2), 295–303.

[8] Hamamori Y, Wu HY, Sartorelli V, and Kedes L (1997). The basic domain of myogenic basic helix–loop–helix (bHLH) proteins is the novel target for direct inhibition by another bHLH protein, Twist. *Mol Cell Biol* **17** (11), 6563–6573.

[9] Spicer DB, Rhee J, Cheung WL, and Lassar AB (1996). Inhibition of myogenic bHLH and MEF2 transcription factors by the bHLH protein Twist. *Science* **272** (5267), 1476–1480.

[10] Maestro R, Dei Tos AP, Hamamori Y, Krasnokutsky S, Sartorelli V, Kedes L, Doglioni C, Beach DH, and Hannon GJ (1999). Twist is a potential oncogene that inhibits apoptosis. *Genes Dev* **13** (17), 2207–2217.

[11] Tamura M and Noda M (1999). Identification of DERMO-1 as a member of helix–loop–helix type transcription factors expressed in osteoblastic cells. *J Cell Biochem* **72** (2), 167–176.

[12] Valsesia-Wittmann S, Magdeleine M, Dupasquier S, Garin E, Jallas AC, Combaret V, Krause A, Leissner P, and Puisieux A (2004). Oncogenic cooperation between H-Twist and N-Myc overrides failsafe programs in cancer cells. *Cancer Cell* **6** (6), 625–630.

[13] Rosivatz E, Becker I, Specht K, Fricke E, Luber B, Busch R, Hofler H, and Becker KF (2002). Differential expression of the epithelial–mesenchymal transition regulators snail, SIP1, and twist in gastric cancer. *Am J Pathol* **161** (5), 1881–1891.

[14] Wang X, Ling MT, Guan XY, Tsao SW, Cheung HW, Lee DT, and Wong YC (2004). Identification of a novel function of TWIST, a bHLH protein, in the development of acquired taxol resistance in human cancer cells. *Oncogene* **23** (2), 474–482.

[15] Yang J, Mani SA, Donaher JL, Ramaswamy S, Itzykson RA, Come C, Savagner P, Gitelman I, Richardson A, and Weinberg RA (2004). Twist, a master regulator of morphogenesis, plays an essential role in tumor metastasis. *Cell* **117** (7), 927–939.

[16] Holland EC (2001). Progenitor cells and glioma formation. *Curr Opin Neurol* **14** (6), 683–688.

[17] Kleihues P, Louis DN, Scheithauer BW, Rorke LB, Reifenberger G, Burger PC, and Cavenee WK (2002). The WHO classification of tumors of the nervous system. *J Neuropathol Exp Neurol* **61** (3), 215–225; discussion 226–229.

[18] Kleihues P and Ohgaki H (1999). Primary and secondary glioblastomas: from concept to clinical diagnosis. *Neuro-Oncology* **1** (1), 44–51.

[19] Chakravarti A, Zhai G, Suzuki Y, Sarkesh S, Black PM, Muzikansky A, and Loeffler JS (2004). The prognostic significance of phosphatidylinositol 3-kinase pathway activation in human gliomas. *J Clin Oncol* **22** (10), 1926–1933.

[20] Guha A and Mukherjee J (2004). Advances in the biology of astrocytomas. *Curr Opin Neurol* **17** (6), 655–662.

[21] Palfi S, Swanson KR, De Bouard S, Chretien F, Oliveira R, Gherardi RK, Kros JM, Peschanski M, and Christov C (2004). Correlation of *in vitro* infiltration with glioma histological type in organotypic brain slices. *Br J Cancer* **91** (4), 745–752.

[22] Yahanda AM, Bruner JM, Donehower LA, and Morrison RS (1995). Astrocytes derived from p53-deficient mice provide a multistep *in vitro* model for development of malignant gliomas. *Mol Cell Biol* **15** (8), 4249–4259.

[23] Bogler O, Nagane M, Gillis J, Huang HJ, and Cavenee WK (1999). Malignant transformation of p53-deficient astrocytes is modulated by environmental cues *in vitro*. *Cell Growth Differ* **10** (2), 73–86.

[24] Kinoshita Y, Jarell AD, Flaman JM, Foltz G, Schuster J, Sopher BL, Irvin DK, Kanning K, Kornblum HI, Nelson PS, et al. (2001). Pescadillo, a novel cell cycle regulatory protein abnormally expressed in malignant cells. *J Biol Chem* **276** (9), 6656–6665.

[25] Peyton M, Stellrecht CM, Naya FJ, Huang HP, Samora PJ, and Tsai MJ (1996). BETA3, a novel helix–loop–helix protein, can act as a negative regulator of BETA2 and MyoD-responsive genes. *Mol Cell Biol* **16** (2), 626–633.

[26] Rostomily RC, Bermingham-McDonogh O, Berger MS, Tapscott SJ, Reh TA, and Olson JM (1997). Expression of neurogenic basic helix–loop–helix genes in primitive neuroectodermal tumors. *Cancer Res* **57** (16), 3526–3531.

[27] Kozak M (1987). An analysis of 5′-noncoding sequences from 699 vertebrate messenger RNAs. *Nucleic Acids Res* **15** (20), 8125–8148.

[28] Dignam JD, Lebovitz RM, and Roeder RG (1983). Accurate transcription initiation by RNA polymerase II in a soluble extract from isolated mammalian nuclei. *Nucleic Acids Res* **11** (5), 1475–1489.

[29] Morrison RS and de Vellis J (1981). Growth of purified astrocytes in a chemically defined medium. *Proc Natl Acad Sci USA* **78** (11), 7205–7209.

[30] Lee MS, Lowe GN, Strong DD, Wergedal JE, and Glackin CA (1999). TWIST, a basic helix–loop–helix transcription factor, can regulate the human osteogenic lineage. *J Cell Biochem* **75** (4), 566–577.

[31] Wang SM, Coljee VW, Pignolo RJ, Rotenberg MO, Cristofalo VJ, and Sierra F (1997). Cloning of the human twist gene: its expression is retained in adult mesodermally-derived tissues. *Gene* **187** (1), 83–92.

[32] Brodeur GM (2003). Neuroblastoma: biological insights into a clinical enigma. *Nat Rev Cancer* **3** (3), 203–216.

[33] Pomeroy SL, Tamayo P, Gaasenbeek M, Sturla LM, Angelo M, McLaughlin ME, Kim JY, Goumnerova LC, Black PM, Lau C, et al. (2002). Prediction of central nervous system embryonal tumour outcome based on gene expression. *Nature* **415** (6870), 436–442.

[34] Bogler O, Huang HJ, and Cavenee WK (1995). Loss of wild-type p53 bestows a growth advantage on primary cortical astrocytes and facilitates their *in vitro* transformation. *Cancer Res* **55** (13), 2746–2751.

[35] Dupont J, Fernandez AM, Glackin CA, Helman L, and LeRoith D (2001). Insulin-like growth factor 1 (IGF-1)–induced twist expression is involved in the anti-apoptotic effects of the IGF-1 receptor. *J Biol Chem* **276** (28), 26699–26707.

[36] Leshem Y, Spicer DB, Gal-Levi R, and Halevy O (2000). Hepatocyte growth factor (HGF) inhibits skeletal muscle cell differentiation: a role for the bHLH protein twist and the cdk inhibitor p27. *J Cell Physiol* **184** (1), 101–109.

[37] Davis FG, Freels S, Grutsch J, Barlas S, and Brem S (1998). Survival rates in patients with primary malignant brain tumors stratified by patient age and tumor histological type: an analysis based on Surveillance, Epidemiology, and End Results (SEER) data, 1973–1991. *J Neurosurg* **88** (1), 1–10.

[38] Wrensch M, Minn Y, Chew T, Bondy M, and Berger MS (2002). Epidemiology of primary brain tumors: current concepts and review of the literature. *Neuro-Oncology* **4** (4), 278–299.

[39] Dai C and Holland EC (2003). Astrocyte differentiation states and glioma formation. *Cancer J* **9** (2), 72–81.

[40] Zhu Y and Parada LF (2002). The molecular and genetic basis of neurological tumours. *Nat Rev Cancer* **2** (8), 616–626.

[41] Pathak S (2002). Organ- and tissue-specific stem cells and carcinogenesis. *Anticancer Res* **22** (3), 1353–1356.

[42] O'Rourke MP and Tam PP (2002). Twist functions in mouse development. *Int J Dev Biol* **46** (4), 401–413.

[43] Funato N, Ohtani K, Ohyama K, Kuroda T, and Nakamura M (2001). Common regulation of growth arrest and differentiation of osteoblasts by helix–loop–helix factors. *Mol Cell Biol* **21** (21), 7416–7428.

[44] Howe LR, Watanabe O, Leonard J, and Brown AM (2003). Twist is up-regulated in response to Wnt1 and inhibits mouse mammary cell differentiation. *Cancer Res* **63** (8), 1906–1913.

[45] Hamamori Y, Sartorelli V, Ogryzko V, Puri PL, Wu HY, Wang JY, Nakatani Y, and Kedes L (1999). Regulation of histone acetyltransferases p300 and PCAF by the bHLH protein twist and adenoviral oncoprotein E1A. *Cell* **96** (3), 405–413.

[46] Gullaud M, Delanoue R, and Silber J (2003). A *Drosophila* model to study the functions of TWIST orthologs in apoptosis and proliferation. *Cell Death Differ* **10** (6), 641–651.

[47] Klaunig JE and Kamendulis LM (2004). The role of oxidative stress in carcinogenesis. *Annu Rev Pharmacol Toxicol* **44,** 239–267.

[48] Kuruganti PA, Wurster RD, and Lucchesi PA (2002). Mitogen activated protein kinase activation and oxidant signaling in astrocytoma cells. *J Neuro-Oncol* **56** (2), 109–117.

[49] Tada M, Iggo RD, Waridel F, Nozaki M, Matsumoto R, Sawamura Y, Shinohe Y, Ikeda J, and Abe H (1997). Reappraisal of p53 mutations in human malignant astrocytic neoplasms by p53 functional assay: comparison with conventional structural analyses. *Mol Carcinog* **18** (3), 171–176.

[50] Nozaki M, Tada M, Kobayashi H, Zhang CL, Sawamura Y, Abe H, Ishii N, and Van Meir EG (1999). Roles of the functional loss of *p53* and other genes in astrocytoma tumorigenesis and progression. *Neuro-Oncology* **1** (2), 124–137.

[51] Kato H, Kato S, Kumabe T, Sonoda Y, Yoshimoto T, Han SY, Suzuki T, Shibata H, Kanamaru R, and Ishioka C (2000). Functional evaluation of *p53* and *PTEN* gene mutations in gliomas. *Clin Cancer Res* **6** (10), 3937–3943.

[52] Jensen NA, Pedersen KM, Lihme F, Rask L, Nielsen JV, Rasmussen TE, and Mitchelmore C (2003). Astroglial c-Myc overexpression predisposes mice to primary malignant gliomas. *J Biol Chem* **278** (10), 8300–8308.

[53] Hayashi S, Yamamoto M, Ueno Y, Ikeda K, Ohshima K, Soma G, and Fukushima T (2001). Expression of nuclear factor-kappa B, tumor necrosis factor receptor type 1, and c-Myc in human astrocytomas. *Neurol Med Chir (Tokyo)* **41** (4), 187–195.

[54] Thiery JP (2002). Epithelial–mesenchymal transitions in tumour progression. *Nat Rev Cancer* **2** (6), 442–454.

[55] Koochekpour S, Jeffers M, Rulong S, Taylor G, Klineberg E, Hudson EA, Resau JH, and Vande Woude GF (1997). Met and hepatocyte growth factor/scatter factor expression in human gliomas. *Cancer Res* **57** (23), 5391–5398.

[56] Hirano H, Lopes MB, Laws ER Jr, Asakura T, Goto M, Carpenter JE, Karns LR, and VandenBerg SR (1999). Insulin-like growth factor-1 content and pattern of expression correlates with histopathologic grade in diffusely infiltrating astrocytomas. *Neuro-Oncology* **1** (2), 109–119.

[57] Merrill MJ and Edwards NA (1990). Insulin-like growth factor-I receptors in human glial tumors. *J Clin Endocrinol Metab* **71** (1), 199–209.

[58] Bowers DC, Fan S, Walter KA, Abounader R, Williams JA, Rosen EM, and Laterra J (2000). Scatter factor/hepatocyte growth factor protects against cytotoxic death in human glioblastoma *via* phosphatidylinositol 3-kinase– and AKT-dependent pathways. *Cancer Res* **60** (15), 4277–4283.

[59] Abounader R, Lal B, Luddy C, Koe G, Davidson B, Rosen EM, and Laterra J (2002). *In vivo* targeting of SF/HGF and c-met expression

via U1snRNA/ribozymes inhibits glioma growth and angiogenesis and promotes apoptosis. *FASEB J* **16** (1), 108–110.

[60] Wick W, Grimmel C, Wild-Bode C, Platten M, Arpin M, and Weller M (2001). Ezrin-dependent promotion of glioma cell clonogenicity, motility, and invasion mediated by BCL-2 and transforming growth factor-beta2. *J Neurosci* **21** (10), 3360–3368.

[61] Yamamoto S, Wakimoto H, Aoyagi M, Hirakawa K, and Hamada H (1997). Modulation of motility and proliferation of glioma cells by hepatocyte growth factor. *Jpn J Cancer Res* **88** (6), 564–577.

[62] Wick W, Platten M, and Weller M (2001). Glioma cell invasion: regulation of metalloproteinase activity by TGF-beta. *J Neuro-Oncol* **53** (2), 177–185.

[63] Chakravarti A, Loeffler JS, and Dyson NJ (2002). Insulin-like growth factor receptor I mediates resistance to anti–epidermal growth factor receptor therapy in primary human glioblastoma cells through continued activation of phosphoinositide 3-kinase signaling. *Cancer Res* **62** (1), 200–207.

[64] Meng Q, Xu J, Goldberg ID, Rosen EM, Greenwald RA, and Fan S (2000). Influence of chemically modified tetracyclines on proliferation, invasion and migration properties of MDA-MB-468 human breast cancer cells. *Clin Exp Metastasis* **18** (2), 139–146.

[65] Wu CJ, O'Rourke DM, Feng GS, Johnson GR, Wang Q, and Greene MI (2001). The tyrosine phosphatase SHP-2 is required for mediating phosphatidylinositol 3-kinase/Akt activation by growth factors. *Oncogene* **20** (42), 6018–6025.

[66] Joy AM, Beaudry CE, Tran NL, Ponce FA, Holz DR, Demuth T, and Berens ME (2003). Migrating glioma cells activate the PI3-K pathway and display decreased susceptibility to apoptosis. *J Cell Sci* **116** (Pt 21), 4409–4417.

[67] Lee MS, Lowe G, Flanagan S, Kuchler K, and Glackin CA (2000). Human Dermo-1 has attributes similar to twist in early bone development. *Bone* **27** (5), 591–602.

[68] Gitelman I (1997). Twist protein in mouse embryogenesis. *Dev Biol* **189** (2), 205–214.

[69] Wolf C, Thisse C, Stoetzel C, Thisse B, Gerlinger P, and Perrin-Schmitt F (1991). The *M-twist* gene of *Mus* is expressed in subsets of mesodermal cells and is closely related to the *Xenopus X-twi* and the *Drosophila twist* genes. *Dev Biol* **143** (2), 363–373.

[70] Ohgaki H, Dessen P, Jourde B, Horstmann S, Nishikawa T, Di Patre PL, Burkhard C, Schuler D, Probst-Hensch NM, Maiorka PC, et al. (2004). Genetic pathways to glioblastoma: a population-based study. *Cancer Res* **64** (19), 6892–6899.